Wavelength characterization of an acousto-optic notch filter for unpolarized near-infrared light

Jean-Claude Kastelik, Justine Champagne, Samuel Dupont, Konstantin B. Yushkov

Wavelength characterization of an acousto-optic notch filter for unpolarized near-infrared light

Jean-Claude Kastelik,[1,*] Justine Champagne,[1] Samuel Dupont,[1] and Konstantin B.Yushkov[2]

[1]*Univ. Valenciennes, CNRS, Univ. Lille, YNCREA, Centrale Lille, UMR 8520 IEMN, DOAE, 59313 Valenciennes, France*

[2]*Acousto-Optical Research Center, National University of Science and Technology "MISIS," 4 Leninsky Prospekt, 119049 Moscow, Russia*

**Corresponding author: Jean-Claude.Kastelik@univ-valenciennes.fr*

A cascaded system of two acousto-optical cells is proposed and experimentally demonstrated for optical notch rejection filtering in the spectral range from 1400 nm to 1600 nm. Two similar paratellurite acousto-optical devices for unpolarized light are used in a free-space gap of a fiber line. Compensation for birefringence in aniso-tropic paratellurite devices provides a diffraction regime that is insensitive to polarization of light. High extinction ratios up to 40 dB are measured.

OCIS codes: (230.1040) Acousto-optical devices; (230.7408) Wavelength filtering devices; (260.1440) Birefringence; (130.5440) Polarization-selective devices.

1. INTRODUCTION

Acousto-optic tunable filters (AOTFs) are well known for spectral and spatial filtering of light [1,2]. Tangential paratellurite-based acousto-optic cells (AOCs) provide performing tunable devices, and a number of commercially efficient AOTFs are available [3]. However, the light diffraction by ultrasound in birefringent media is strongly dependent on the polarization of incident light, with the main consequence of reducing the optical transmission. Also well known is the possibility of AO anisotropic interaction of unpolarized light with the use of a special geometry of diffraction, which is based on a simultaneous diffraction of ordinary and extraordinary beams into opposite diffraction orders [4–6]. Independent filtering of the two orthogonal polarizations of the optical beam can be obtained by cascaded similar AOCs [7–9]. Each cell of the tandem controls one of the eigen polarizations of light in the crystal. The transmitted beam is also split into two orthogonal polarization modes because of birefringence of the material. At the output of the cell, the transmitted beam remains split into two orthogonally polarized beams, which is not suitable for a notch rejection optical filter. This kind of filtering is largely applied in the field of telecommunications and instrumentation [10–14].

In this paper, we consider a notch filtering configuration of anisotropic diffraction with polarization splitting in a tandem of similar AOCs for unpolarized light. This "double filtering" configuration is obtained when the same RF frequency is applied to both cells providing higher contrast and rejection rate [15].

The optical architecture was extensively described in a previously published paper [16] for application in optical communication networks [17] with the use of wavelength-division multiplexing (WDM) technology for control and equalization of multichannel light beams.

We propose a quite different use of this cascaded AO system for a tunable optical notch rejection filter with a high extinction ratio.

First, we summarize the operation principle of this multi-purpose system and its main design parameters. Then, we focus on a single frequency operation mode for optical notch filtering. Experimental results are presented with near-infrared (NIR) input light in the optical band from 1400 nm to 1600 nm. Two configurations are studied, considering the incident light a discrete or continuous optical spectrum. A high extinction ratio up to 40 dB was measured for the optical notch filter in a wide optical bandwidth.

2. PRINCIPLE OF OPERATION

Based on our previous paper [16], the general scheme of beam traces and orientation of the cells is presented in Fig. 1, assuming a polychromatic unpolarized input light beam (wavelengths $\lambda_1, \lambda_2 \ldots \lambda_i$). All the optical facets of the devices are perpendicular to the direction of the input light beam. In the first AOC 1, due to the optical anisotropy of the TeO_2 crystal, the multi-wavelength arbitrary polarized incident beam is split into two propagation modes orthogonally polarized: the extraordinary "e" mode and the ordinary "o" mode.

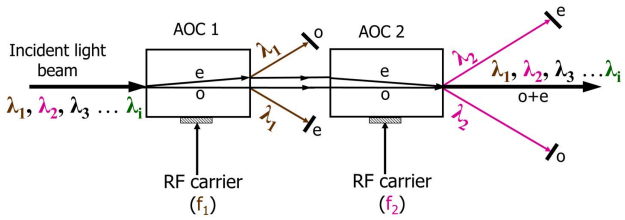

Fig. 1. Optical scheme of cascaded attenuator of unpolarized light.

At the output of AOC 1, these beams are then separated and parallel. The second AOC 2 compensates for the birefringence effect in the first crystal because it is placed symmetrically to the first one. Thus, the extraordinarily polarized beam is shifted by the second crystal to the same distance as by the first crystal but in the opposite direction. The "e" and "o" optical modes are then recombined "o+e" at the output of AOC 2.

Moreover, the two devices have the same AO characteristics, in particular the tuning relation. As, e.g., tuning the ultrasonic frequency f_1 on AOC 1 leads to the simultaneous diffraction of the two optical modes of the wavelength λ_1. More precisely, as the interaction takes place with a shear ultrasonic wave, the input "e" mode is up-diffracted and becomes an "o" mode, and the input "o" mode is down-diffracted as an "e" mode. These two diffracted beams are then stopped. By a proper modulation of the ultrasonic driving power, the optical power of the transmitted beam at wavelength λ_1 can be reduced in a range from 0 to 20 dB compared to the input optical power at the same wavelength. The same configuration is obviously obtained for all the optical wavelengths by tuning the ultrasonic frequency: f_1 for λ_1, f_2 for $\lambda_2 \ldots f_i$ for λ_i. This operating mode for AOC 1 is also valid for AOC 2, except that the polarizations of the diffracted modes are permuted because the second crystal is placed symmetrically to the first one. The two AOCs operate independently.

This optical AO system is mainly used in a multichannel configuration as a tunable optical attenuator, depicted in Fig. 2.

Assuming several wavelengths with different optical powers at the input, the ultrasonic frequency carriers are applied to the AOCs in order to equalize the optical powers of all the wavelengths at the output. Tuning the ultrasonic frequency and the driving powers results in adjusting the wavelength and the optical power of the corresponding transmitted light. All the extraordinary and ordinary diffracted beams are stopped. As, e.g., Fig. 2 shows four wavelengths at the input of AOC 1.

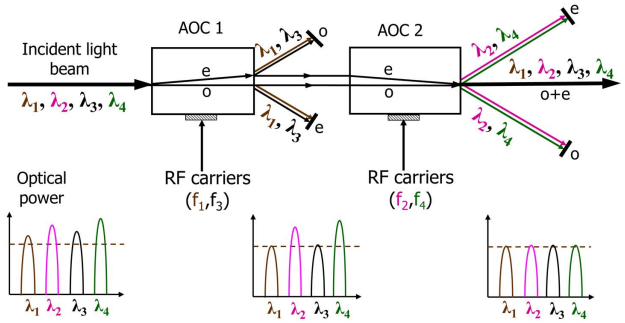

Fig. 2. Multichannel operation mode.

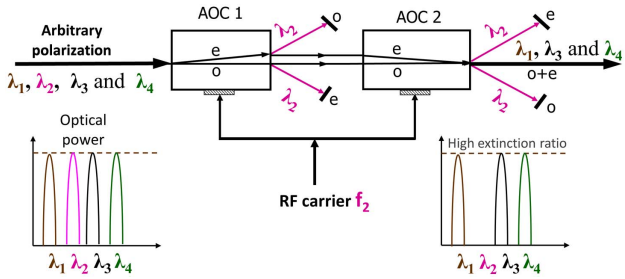

Fig. 3. Principle of operation of the AOTNF.

In order to reduce the inter-channel crosstalks, the operating frequencies are distributed among the two cells instead of a single one. RF carriers f_1 and f_3 are applied to AOC 1, as well as RF carriers f_2 and f_4 are applied to AOC 2. The corresponding driving powers are adjusted in order to equalize the optical powers at the output. All the wavelengths can be independently attenuated with an extinction ratio up to 16 dB in practice.

In the present paper, we consider a specific single ultrasonic frequency operating mode as depicted in Fig. 3. The same ultrasonic frequency, as, e.g., f_2 for the wavelength λ_2, is applied simultaneously to the piezo-transducers of AOC 1 and AOC 2. This cascaded system, AO tunable notch filter (AOTNF), of two AO attenuators allows to achieve high extinction of the selected wavelength up to 40 dB.

3. DESIGN OF THE ACOUSTO-OPTIC CELLS

We summarize the main characteristics of the AOCs, which were extensively presented in our previous paper, especially concerning the configurations of anisotropic interaction. In order to obtain both a high diffraction efficiency and good spectral resolution, we designed paratellurite-based AO cells with the cut angle $\alpha = 10°$. Numerical calculations of the ultrasonic frequencies for the two extraordinary to ordinary modes and ordinary to extraordinary modes anisotropic interactions are given in Fig. 4. A large optical bandwidth from 1200 nm to 1700 nm is considered. For each wavelength, the angle of intersection of the curves corresponding to the double diffraction is identical and equal to 22° from the optical axis of the crystal. As the device operates in the wavelength range 1200–1700 nm,

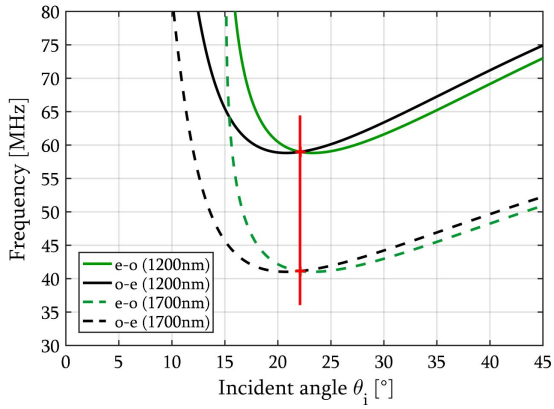

Fig. 4. Determination of the point of operation of the AONTF.

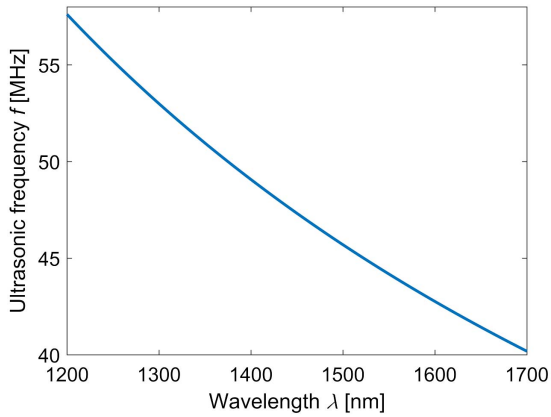

Fig. 5. Tuning relation of the AOTNF.

the dispersion of the refractive indices is negligibly small, and it does not influence the operating point in the AONTF. As a consequence, additional adjustment of the crystal when tuning the device becomes not so necessary. Then, Fig. 5 shows the tuning relation for the double interaction operating mode. Generation of ultrasound with the efficiency 50% and higher is provided in the range of RF signals from 40 MHz to 60 MHz.

Diffraction efficiencies in the AO cells and spectral resolutions were measured separately at the frequencies $f_1 = 45.4$ MHz, $f_2 = 44.8$ MHz, $f_3 = 44.2$ MHz, and $f_4 = 43.6$ MHz, which corresponded to the wavelengths of the diode lasers used for experimental validation of the tunable notch filter presented in the next section. The obtained spectrograms are presented in Fig. 6 with solid curves for AOC 1 and dashed curves for AOC 2. The driving power necessary for providing diffraction efficiency of 95% is less than approximately 2.0 W for the longest wavelength of the tuning range. For a shorter wavelength, the optimal driving power is lower due to a wavelength squared dependence. In the same way, the two devices had a piezo-transducer length equal to 12 mm,

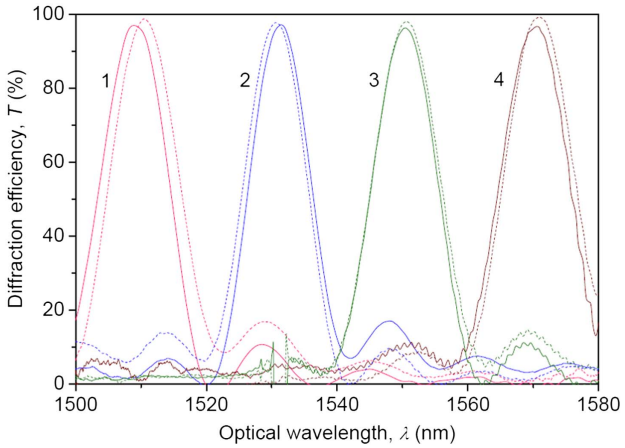

Fig. 6. Diffraction efficiency in both cells (solid curves for AOC 1 and dashed curves or AOC 2) at four independent channels: 1—$f_1 = 45.4$ MHz, 2—$f_2 = 44.8$ MHz, 3—$f_3 = 44.2$ MHz, and 4—$f_4 = 43.6$ MHz.

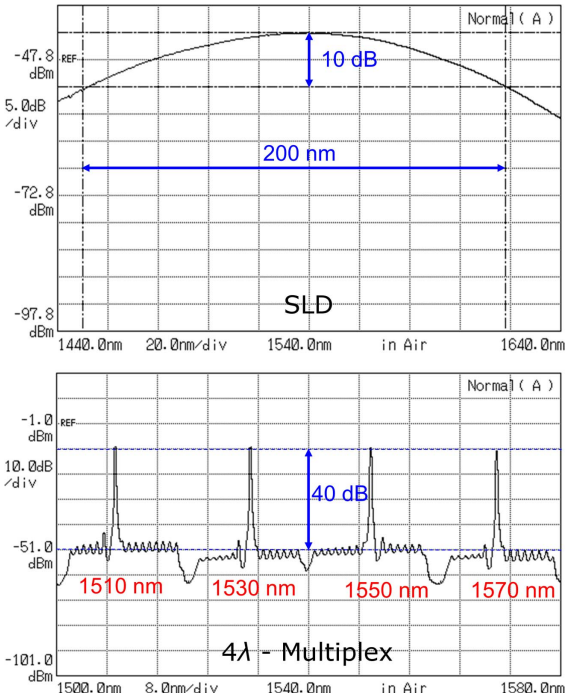

Fig. 7. Optical characteristics of SLD and 4-λ multiplex.

and the measured full width at half-maximum (FWHM) spectral bandwidths are in the range 10–12 nm.

Usage of the filter as an attenuator of light in the zeroth diffraction order determines configuration of the cells: both

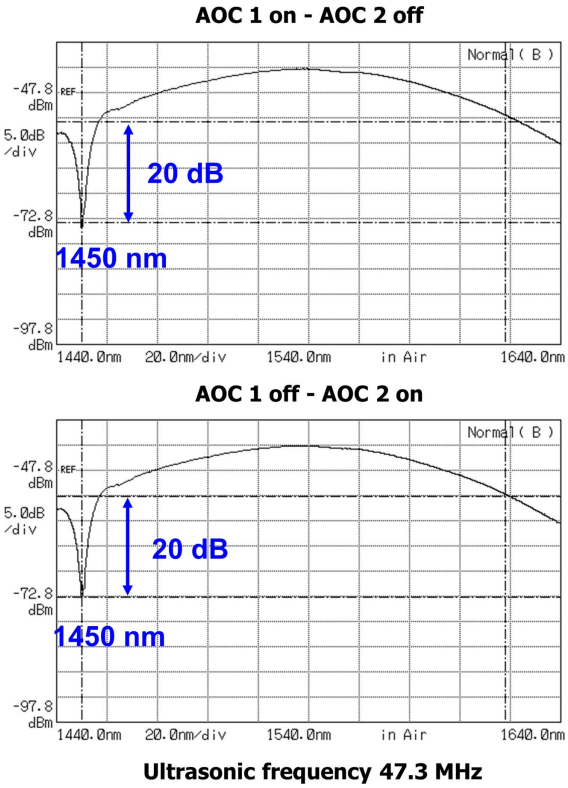

Fig. 8. Maximal attenuation for $\lambda = 1450$ nm.

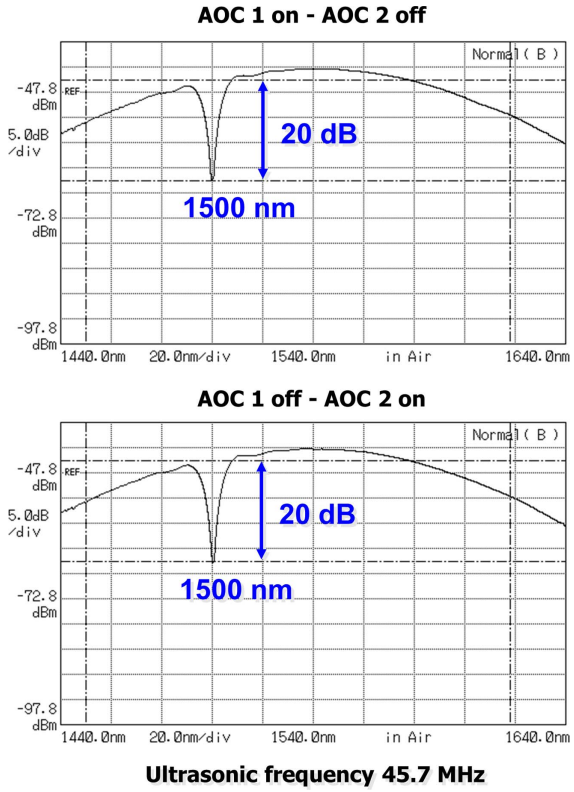

Fig. 9. Maximal attenuation for $\lambda = 1500$ nm.

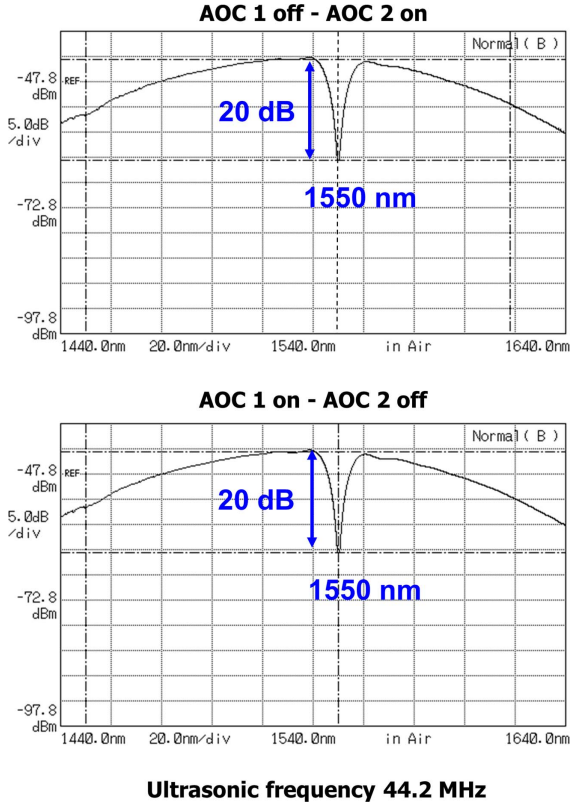

Fig. 10. Maximal attenuation for $\lambda = 1550$ nm.

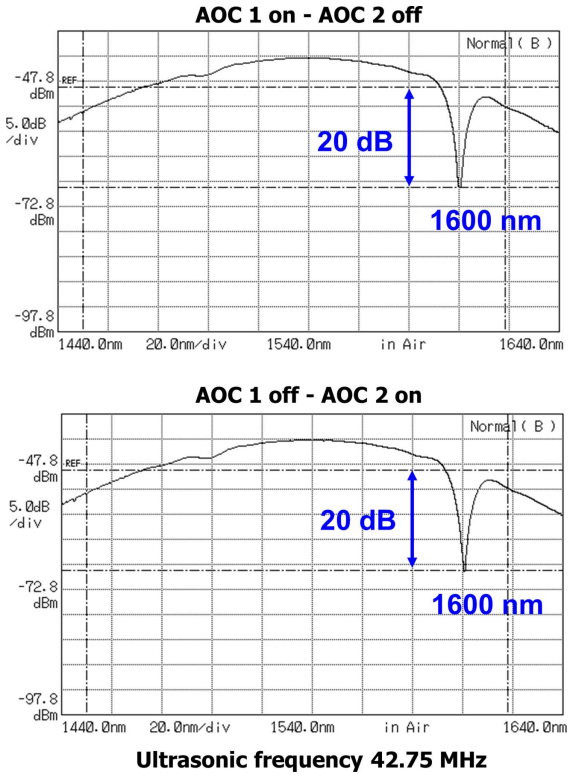

Fig. 11. Maximal attenuation for $\lambda = 1600$ nm.

input and output optical facets are cut orthogonally to the beam with antireflection coatings. Maximum reflectivity per surface in the cells is less than 0.3% in the range of wavelength from 1250 nm to 1550 nm. A requirement of precise compensation for birefringence needs similarity of optical properties of both AOCs. To provide this, the cells have been produced from a single bulk crystal of paratellurite after cutting the optical facets and welding the piezo transducers onto the crystal. As a result, overall optical insertion losses did not exceed 2 dB. The optical walk-off angle of an extraordinarily polarized wave in the crystal is equal to $\beta = 2.4°$, so at the output of the first cell, the distance between the axes of the adjacent beams is equal to 1.1 mm. This magnitude is comparable to the width of the beams; therefore, an extraordinarily polarized component of the incident light may be lost if the shift is not compensated.

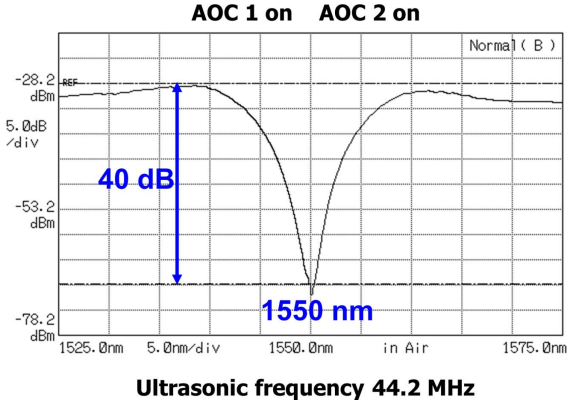

Fig. 12. Maximal attenuation of the AOTNF for $\lambda = 1550$ nm.

4. EXPERIMENTAL VALIDATION

The main goal of the experiment was to test the setup in the NIR spectral range for two types of sources: the first with a continuous light spectrum and the second with multiplexed single wavelengths. For this purpose, we used an optical spectrum analyzer (OSA Anritsu MS9710C), including a super luminescent laser diode (SLD) source emitting from 1440 nm to 1640 nm with a maximum (−43 dBm) at 1540 nm, as shown in Fig. 7. We also used a discrete light spectrum issued from four 20 nm spaced laser diodes passing through a multiplexer (4-λ multiplex, AFOP 4-channels CWDM) as can be seen in Fig. 7.

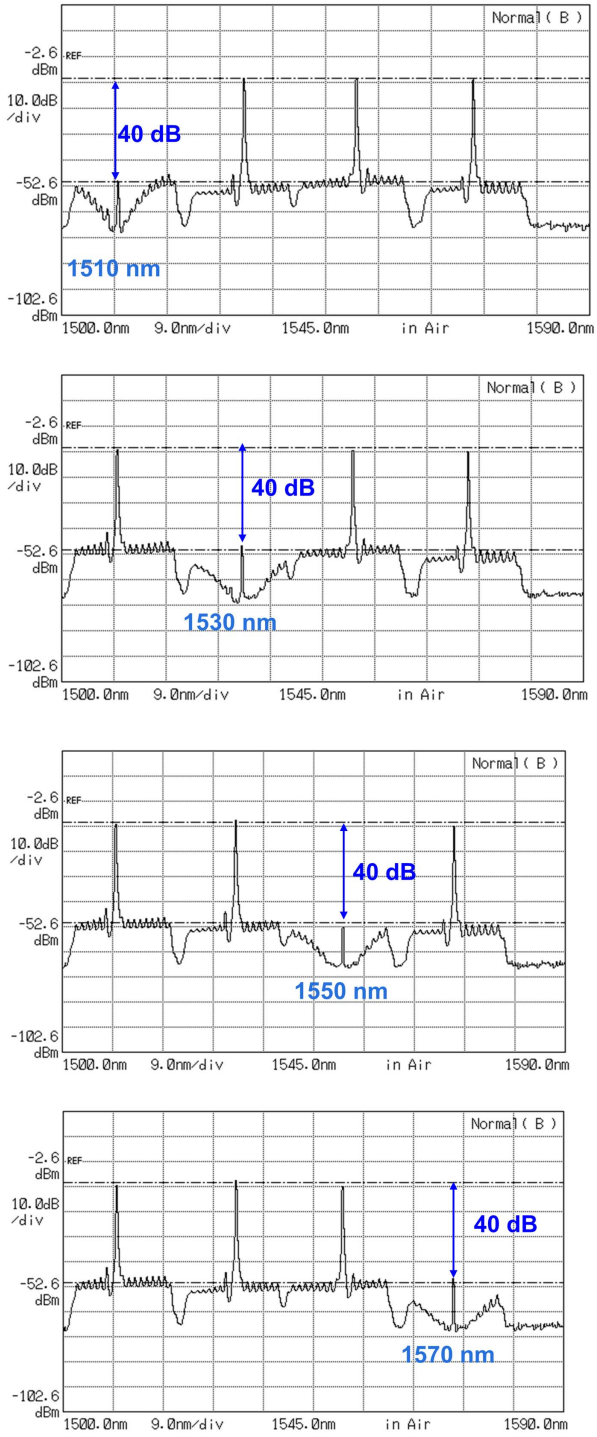

Fig. 13. Demonstration of 40 dB extinction for all the carriers of 4-λ multiplex.

In a first phase, we checked the wavelength tunability and measured the attenuation efficiencies of the zeroth order for either AOC 1 or for AOC 2. Figures 8–11 show that whatever the wavelength of the SLD source or the AOC, attenuation up to 20 dB is obtained. In all cases, the driving power is less than 2 W.

Then, the single ultrasonic frequency was applied simultaneously to the two AOCs. Figure 12 shows a maximum attenuation of 40 dB for the wavelength 1550 nm.

As the optical level of power of the SLD is relatively low (less than −43 dBm), we encountered some difficulties to measure precisely the maximum attenuation possible for other wavelengths due to the minimum of the level range (−90 dBm) of OSA. This is why we present these results considering the discrete optical spectrum presented above. The optical powers of the four optical carriers were adjusted with a fixed value: almost −13 dBm. A maximum attenuation of 40 dB is then clearly demonstrated (Fig. 13) for all these wavelengths: 1510 nm, 1530 nm, 1550 nm, and 1570 nm.

5. CONCLUSION

In this paper, we presented a specific operating mode of a cascaded system of two AO devices. As a single ultrasonic frequency is applied simultaneously to the two cells, a double-filtering configuration is achieved. Moreover, as the interaction takes place in a double diffraction mode, high diffraction is obtained, whatever the polarization of the input light. We consider the transmitted beam of the system in order to realize a tunable notch rejection filter. Experimental results were presented with NIR input light from optical sources available in the optical band from 1400 nm to 1600 nm. A high extinction ratio up to 40 dB was measured.

Funding. Russian Foundation for Basic Research (RFBR) (15-07-04512-A).

Acknowledgment. This paper is based on the talk presented at the 13th School on Acousto-Optics and Applications, Moscow, Russia, 19–23 June 2017. J. C. Kastelik, Acousto-optic notch filter for unpolarized near-infrared light. Program and Abstracts Book, p. 16.

REFERENCES

1. J. Xu and R. Stroud, *Acousto-Optic Devices: Principles, Design, and Applications* (Wiley, 1992).
2. A. Goutzoulis and D. Pape, *Design and Fabrication of Acousto-Optic Devices* (Marcel Dekker, 1994).
3. I. C. Chang, "Acousto-optic tunable filters," Opt. Eng. **20**, 824–829 (1981).
4. H. Lee, "Polarization independent acousto-optic light modulation with large angular aperture," Appl. Opt. **27**, 815–817 (1988).
5. V. B. Voloshinov and V. Y. Molchanov, "Acousto-optic modulation of radiation with arbitrary polarization direction," Opt. Laser Technol. **27**, 307–313 (1995).
6. V. B. Voloshinov, V. Y. Molchanov, and T. M. Babkina, "Acousto-optic filter of nonpolarized electromagnetic radiation," Tech. Phys. **45**, 1186–1191 (2000).

7. S. N. Antonov, “Acoustooptic nonpolar light controlling devices and polarization modulators based on paratellurite crystals,” Tech. Phys. **49**, 1329–1334 (2004).
8. L. N. Magdich, K. B. Yushkov, and V. B. Voloshinov, “Wide-aperture diffraction of unpolarised radiation in a system of two acousto-optic filters,” Quantum Electron. **39**, 347–352 (2009).
9. K. B. Yushkov, S. Dupont, J.-C. Kastelik, and V. B. Voloshinov, “Polarization-independent imaging with an acousto-optic tandem system,” Opt. Lett. **35**, 1416–1418 (2010).
10. H. S. Kim, S. H. Yun, I. K. Hwang, and B. Y. Kim, “All-fiber acousto-optic tunable notch filter with electronically controllable spectral profile,” Opt. Lett. **22**, 1476–1478 (1997).
11. K. J. Lee, D.-I. Yeom, and B. Y. Kim, “Narrowband, polarization insensitive all-fiber acousto-optic tunable bandpass filter,” Opt. Express **15**, 2987–2992 (2007).
12. J. C. Carter, S. M. Angel, M. Lawrence-Snyder, J. Scaffidi, R. E. Whipple, and J. G. Reynolds, “Standoff detection of high explosive materials at 50 meters in ambient light conditions using a small Raman instrument,” Appl. Spectrosc. **59**, 769–775 (2005).
13. W. Zhang, F. Gao, F. Bo, Q. Wu, G. Zhang, and J. Xu, “All-fiber acousto-optic tunable notch filter with a fiber winding driven by a cuneal acoustic transducer,” Opt. Lett. **36**, 271–273 (2011).
14. H.-H. Lu, C.-Y. Li, T.-C. Lu, C.-J. Wu, C.-A. Chu, A. Shiva, and T. Mochii, “Bidirectional fiber-wireless and fiber-VLLC transmission system based on an OEO-based BLS and a RSOA,” Opt. Lett. **41**, 476–479 (2016).
15. V. E. Pozhar and V. I. Pustovoit, “Consecutive collinear diffraction of light in several acoustooptic cells,” Sov. J. Quantum Electron. **15**, 1438–1439 (1985).
16. J.-C. Kastelik, K. B. Yushkov, S. Dupont, and V. B. Voloshinov, “Cascaded acousto-optical system for the modulation of unpolarized light,” Opt. Express **17**, 12767–12776 (2009).
17. J. Sapriel, D. Charissoux, V. B. Voloshinov, and V. Y. Molchanov, “Tunable acousto-optic filters and equalizers for WDM applications,” J. Lightwave Technol. **20**, 892–899 (2002).